

# Minocycline Attenuates High Mobility Group Box 1 Translocation, Microglial Activation, and Thalamic Neurodegeneration after Traumatic Brain Injury in Post-Natal Day 17 Rats

Dennis W. Simon,<sup>1,2,7</sup> Rajesh K. Aneja<sup>1,2</sup> Henry Alexander,<sup>7</sup> Michael J. Bell,<sup>1,3</sup>  
Hülya Bayır,<sup>1,5</sup> Patrick M. Kochanek,<sup>1,2,4,7</sup> and Robert S.B. Clark<sup>1,2,4,6,7</sup>

## Abstract

In response to cell injury, the danger signal high mobility group box-1 (HMGB) is released, activating macrophages by binding pattern recognition receptors. We investigated the role of the anti-inflammatory drug minocycline in attenuating HMGB1 translocation, microglial activation, and neuronal injury in a rat model of pediatric traumatic brain injury (TBI). Post-natal day 17 Sprague-Dawley rats underwent moderate-severe controlled cortical impact (CCI). Animals were randomized to treatment with minocycline (90 mg/kg, intraperitoneally) or vehicle (saline) at 10 min and 20 h after injury. Sham received anesthesia and craniotomy. We analyzed HMGB1 translocation (protein fractionation and Western blotting), microglial activation (Iba-1 immunohistochemistry), neuronal death (Fluoro-Jade-B [FJB] immunofluorescence), and neuronal cell counts (unbiased stereology). Behavioral assessments included motor and Morris-water maze testing. Nuclear to cytosolic translocation of HMGB1 in the injured brain was attenuated in minocycline versus vehicle-treated rats at 24 h ( $p < 0.001$ ). Treatment with minocycline reduced microglial activation in the ipsilateral cortex, hippocampus, and thalamus ( $p < 0.05$  vs. vehicle, all regions); attenuated neurodegeneration (FJB-positive neurons) at seven days ( $p < 0.05$  vs. vehicle); and increased thalamic neuronal survival at 14 days (naïve  $22773 \pm 1012$  cells/mm<sup>3</sup>, CCI + vehicle  $11753 \pm 464$ , CCI + minocycline  $17047 \pm 524$ ;  $p < 0.001$ ). Minocycline-treated rats demonstrated delayed motor recovery early after injury but had no injury effect on Morris-water maze whereas vehicle-treated rats performed worse than sham on the final two days of testing (both  $p < 0.05$  vs. vehicle). Minocycline globally attenuated HMGB1 translocation and microglial activation in injured brain in a pediatric TBI model and afforded selective thalamic neuroprotection. The HMGB1 translocation and thalamic injury may represent novel mechanistic and regional therapeutic targets in pediatric TBI.

**Keywords:** HMGB1; microglia; minocycline; neuroinflammation; traumatic brain injury

## Introduction

PEDIATRIC TRAUMATIC BRAIN INJURY (TBI) accounts for more than 50,000 hospitalizations per year and is a leading cause of death and permanent disability in children.<sup>1</sup> The developing brain appears particularly susceptible to poor outcomes after TBI.<sup>2,3</sup> A dysregulated immune response observed in children after TBI<sup>4,5</sup> could result in secondary neuronal injury and contribute to impaired neurological outcomes in children. Indeed, studies of post-traumatic neuroinflammation have shown age-dependent differences, with increased inflammation observed at the extremes of

age<sup>4,6,7</sup>; several markers of neuroinflammation have been associated with poor outcome in children with severe TBI.<sup>4,5,8,9</sup>

Damage-associated molecular patterns (DAMPs) are molecules released from dead or stressed cells and are capable of initiating or propagating an immune response.<sup>10</sup> The prototypical DAMP, high mobility group box-1 (HMGB1), is a nuclear chromatin-binding protein that may be released to the extracellular space by traumatic lysis or necrosis, or translocated to cytosol as a result of hyperacetylation and subsequently released to extracellular space.

The HMGB1 has been detected in the cerebrospinal fluid (CSF) of adult<sup>11</sup> and pediatric<sup>5</sup> patients with severe TBI and appears to be

Departments of <sup>1</sup>Critical Care Medicine, <sup>2</sup>Pediatrics, <sup>3</sup>Neurological Surgery, <sup>4</sup>Anesthesiology, <sup>5</sup>Environmental and Occupational Health, and the <sup>6</sup>Clinical and Translational Science Institute, University of Pittsburgh School of Medicine; and the <sup>7</sup>Safar Center for Resuscitation Research, University of Pittsburgh School of Medicine, Pittsburgh, Pennsylvania.

an early inflammatory mediator, with peak levels occurring within the first 72 h of injury.<sup>11</sup> Extracellular HMGB1 may bind to pattern-recognition receptors such as Toll-like receptor 4 (TLR4) and receptor for advanced glycosylation of end products (RAGE), resulting in a pro-inflammatory macrophage or microglial phenotype.<sup>12</sup> In children with severe TBI, the peak CSF concentration of HMGB1 was shown to be inversely proportional to the Glasgow Outcome Scale (GOS) score at six months.<sup>5</sup> Therefore, attenuating the inflammatory response by attenuating release of HMGB1 may be a therapeutic target after TBI.

Microglial activation may be reduced with minocycline, a second-generation tetracycline antibiotic with anti-inflammatory actions and favorable central nervous system penetration.<sup>13–15</sup> Studies of minocycline in adult TBI models have demonstrated reduced neuroinflammation<sup>15,16</sup> and variable degrees of neuroprotection.<sup>15–17</sup> Limited studies have been performed testing minocycline in pediatric TBI models. In a neonatal repetitive injury model, minocycline demonstrated minimal benefit and potential harm.<sup>18</sup> A closed-head injury model of neonatal TBI evaluating medium-dose minocycline observed altered microglial gene expression in the treatment group but did not evaluate functional outcomes.<sup>19</sup>

The mechanism(s) of minocycline-induced neuroprotection have not been well established in TBI. Several *in vitro* and *in vivo* studies evaluating ischemia-reperfusion models observed that minocycline reduced translocation and extracellular HMGB1, TLR4, and RAGE activation and signaling via nuclear factor- $\kappa$ B.<sup>20–22</sup> It is unclear, however, whether blocking microglial activation and HMGB1 translocation acutely after severe TBI in children will improve outcomes by preventing secondary injury, or worsen outcomes by impeding normal immune-mediated reparative processes.

Using a model of pediatric TBI in post-natal day (PND 17) Sprague-Dawley rats,<sup>23</sup> we administered high-dose minocycline (90 mg/kg intraperitoneally [ip]) at 10 min and 20 h after controlled cortical impact (CCI). We observed significant reduction in HMGB1 translocation to cytoplasm, attenuated microglial activation, reduced neurodegeneration in the thalamus, and improved spatial memory acquisition.

## Methods

### Animals and surgical procedures

Studies were approved by the Institutional Animal Care and Use Committee at the University of Pittsburgh. The PND 17 male Sprague-Dawley rats (35–40 g) were purchased from Harlan (Madison, WI) and allowed to acclimate for at least one week before injury. Animals were housed in litters with their dam in a temperature controlled room with lighting on a 12 h day/night schedule with dams having access to standard chow and water *ad libitum*.

Separate squadrons of rats were used for assessment of HMGB1 translocation ( $n = 3–4$ /group, 10 rats total), seven day immunohistochemical studies ( $n = 3$ /group, nine rats total), and functional outcome and 14 day histological assessment ( $n = 10–11$ /group, 32 rats total).

The CCI model of TBI was performed as described previously.<sup>23</sup> Briefly, animals were anesthetized with 2% isoflurane and 2:1 N<sub>2</sub>O/O<sub>2</sub> blend via nosecone, then placed in a modified stereotactic frame with ear bars to stabilize the head. Core temperature was maintained at 37.5–38°C measured via rectal temperature probe. A 6.5-mm diameter craniotomy was performed in the left parietal bone using a high-speed air drill. The injury was performed for all experiments using a 6-mm diameter impact tip, velocity of 4 m/sec, depth of 2.5 mm, and dwell time of 50 msec. After CCI, the bone flap was replaced and secured with Koldmount dental cement (Vernon-Benshoff, Albany, NY). Shams received anesthesia and craniotomy

without CCI. Pups were allowed to recover in a warmed cubicle and subsequently transferred back to their dams.

### Minocycline treatment

Rats were block randomized after CCI or sham injury to treatment with minocycline or vehicle. Animals randomized to treatment with minocycline (Sigma, St Louis, MO) received 0.9% saline 90 mg/kg ip at 10 min after injury and a second dose of 90 mg/kg ip at 20 h. Rats randomized to vehicle received an equal volume of 0.9% saline ip at the same time points.

### Protein fractionation and Western blotting

At 24 h after injury, PND 17 rats were anesthetized and transcardially perfused with 50 mL of heparinized saline. This time point was chosen to coincide with the peak period of HMGB1 translocation observed in other studies of brain injury.<sup>11,24</sup> The hemisphere ipsilateral to injury was homogenized in a dounce homogenizer with lysis buffer containing 20 mM HEPES (pH 7.8), 10 mM NaCl, 1.5 mM MgCl<sub>2</sub>, 1 mM ethylenediaminetetraacetic acid, 1 mM EGTA, 250 mM sucrose, 1 mM dithiothreitol, 1 mM phenylmethylsulfonyl fluoride, and 2  $\mu$ g/mL aprotinin. The cytosolic fraction was isolated by differential centrifugation using standard technique. Briefly, samples were incubated at 4°C for 30 min, then centrifuged at 3500 rpm for 15 min at 4°C to remove nuclei and cellular debris. The supernatant was collected and centrifuged at 48,000 rpm for 17 min at 4°C to remove the mitochondrial fraction. The supernatant, containing enriched cytosolic protein, was stored at –80°C for further analysis.

Immunoblotting was performed using standard technique. Briefly, samples were thawed and 20  $\mu$ g aliquots, as determined by bicinchoninic acid (BCA) assay, were mixed with 4 $\times$ Laemmli Sample Buffer (BioRad, Hercules, CA), heated at 95°C for 5 min, loaded onto pre-cast TGX 12% gels (Bio-Rad), and proteins separated electrophoretically. Transfer onto polyvinylidene fluoride membranes (PVDF) (Millipore Immobilon, Cat#HSEQ00010, Bedford, MA) was performed at 100V for 75 min at 4°C. The membrane was washed in Tris-buffered saline (TBS; Bio-Rad)-0.1%-Tween-20 (TBST) and blocked 1 h in TBST +5% blotting grade milk (TBS-T/milk).

The membrane was incubated with monoclonal primary antibody against HMGB1 (1:1000; MAB1690, R&D systems, Minneapolis, MN) in TBS-T/milk overnight at 4°C, washed, and then incubated in appropriate secondary antibody in TBS-T/milk for 2 h at room temperature. Blots were incubated with Supersignal West Femto Maximum Sensitivity Substrate (Thermo Scientific, Cat#34095, Rockford, IL), imaged on BioRad Chemi Doc XRS+ imaging system, and band intensity analyzed by ImageLab software (Version 4.0, BioRad). The membrane was then stripped with Restore™ Western Blot Stripping Buffer (ThermoFisher Scientific, Waltham, MA) according to manufacturer instructions and reprobed for  $\beta$ -actin (1:2000, Abcam, Cambridge, MA) and Histone H3 (1:2000, Abcam) using the methods above.

### Functional outcomes

**Motor function.** Rats were assessed for motor function using the beam balance and inclined plane tasks for five days after injury. Before CCI, the rats were pre-trained to remain on a 1.5 cm wide and 90 cm high wooden beam for 60 sec for three consecutive trials. Testing consisted of three trials per day for five days. For the inclined plane, the rats were pre-trained to remain on a wide board set to incline for 10 sec at 70 degrees for three consecutive trials. Post-injury, animals were placed on the board at 45 degrees and the angle was increased in 5-degree increments to a maximum angle of 80 degrees. We recorded the maximum angle at which the rat could remain on the board for 10 sec given three attempts.

**Cognitive function.** Spatial memory acquisition was assessed using the Morris-water maze (MWM) as described previously. Briefly, rats underwent testing on day 10–14 after injury for latency to find the hidden platform. Probe and visible platform trials were performed on day 14 to assess memory retention and for visual deficits. The water maze consists of a pool that is 180 cm in diameter and 60 cm high. The pool was filled with water ( $26 \pm 1^\circ\text{C}$  in temperature) to a depth of 28 cm. A platform that is 10 cm in diameter and set 2 cm below the surface of the water was used as the hidden platform. The pool was located in a  $2.5 \times 2.5$  m room with visual cues that remained constant throughout the experiment.

#### Histological assessment

Seven days after CCI, rats were anesthetized and transcardially perfused with 50 mL heparinized ice-cold saline followed by 50 mL 4% paraformaldehyde in phosphate-buffered saline. The brain was removed and post-fixed in 4% paraformaldehyde for 24 h. Paraffin-embedded brains were cut into  $5\text{-}\mu\text{m}$  coronal sections for immunohistochemistry and immunofluorescence. Fluoro-Jade-B (FJB) staining was performed by removing paraffin in a series of xylene, immersed twice in 100% ethanol (EtOH) and 1% sodium hydroxide (in 80% EtOH) for 90 sec, and then 70% EtOH for 30 sec. Slides were placed on a shaker in 0.06% potassium permanganate for 10 min and washed in distilled water before immersion in a 0.006% working solution of FJB (Histo-Chem Inc., Jefferson, AR) with 4',6-diamidino-2-phenylindole (Sigma, St Louis, MO) for 30 min. Slides were imaged with a Nikon Eclipse 90i microscope.

Iba-1 immunohistochemistry was performed using standard technique. Briefly, sections were deparaffinized and placed in 2%  $\text{H}_2\text{O}_2$  for 20 min and blocked with 3% normal goat serum (Vector, Burlingame, CA) in TBS containing 0.25% Triton X for 1 h. Sections were incubated overnight in TBS-X solution containing rabbit anti-Iba-1 antibody (1:1000, Wako Chemicals, Osaka, Japan). The sections were then incubated for 1 h with anti-rabbit HRP-conjugated secondary antibody (ABC Elite Kit, Vector) and stained with 3,3'-diaminobenzidine (DAB, Vector). Slides were imaged using a Nikon Eclipse 90i microscope and Iba-1 positive objects counted within the ipsilateral hippocampus, thalamus, and cerebral cortex.

**Late histological outcome.** At 14 days after the insult, on completion of MWM testing, the rats were re-anesthetized and perfused as above. The brains were cryoprotected in 15% and 30% sucrose solution and frozen in liquid nitrogen. Serial coronal  $40\text{-}\mu\text{m}$  thick sections were taken every  $160\text{-}\mu\text{m}$  through the entire contusion using a cryotome, mounted on slides, and stained with cresyl violet. Image analysis software (MCID; Imaging Research, Saint Catharines, Ontario, Canada) was used to analyze lesion volumes as described previously.<sup>25</sup>

To assess neuronal loss, unbiased stereology was performed to count the total number of surviving neurons present 14 days after injury. The two-stage combination of optical disector and Cavalieri volume-point counting methods was used as described previously.<sup>26</sup> To generate an unbiased sample, every other section was sampled from eight sections containing the dorsal hippocampus. Stereologer software (Stereology Resource Center, Chester, MD) was used. The optical disector had a size of  $50 \times 50\text{-}\mu\text{m}$ , a height of  $10\text{-}\mu\text{m}$ , and a guard-zone of  $4\text{-}\mu\text{m}$ . A grid spacing of  $500\text{-}\mu\text{m} \times 500\text{-}\mu\text{m}$  in the x- and y-axis was used. The estimated number of surviving neurons in each field was divided by the volume of the region of interest to obtain the neuronal cellular density. Sampling had a coefficient of error  $\leq 0.1$ .

#### Statistical analysis

Statistical analysis was performed using Prism 6 (Graphpad, La Jolla, CA). Behavioral data were analyzed by repeated measures

analysis of variance (ANOVA). When the overall ANOVA revealed a significant effect, the data were further analyzed with the Fisher *post-hoc* test to determine specific group differences. All other data were analyzed by Student *t* test. All data are presented as mean  $\pm$  standard error of the mean. A *p*-value  $< 0.05$  was considered significant.

## Results

### HMGB1 translocation after TBI in PND 17 rats and the effect of minocycline

The nuclear protein HMGB1 has been shown to translocate from the nucleus to the cytoplasm in response to injury where it may be released from cells and contribute to the pathogenesis of various inflammatory diseases.<sup>12</sup> Previous reports have found peak CSF HMGB1 concentration is associated with unfavorable neurological outcome in children with severe TBI. We therefore investigated HMGB1 translocation in a CCI model of pediatric TBI.

The PND 17 Sprague Dawley rats were randomized to minocycline 90 mg/kg ip at 10 min and 20 h after injury or an equivalent volume of physiologic saline. At 24 h after injury, animals were sacrificed, the ipsilateral hemisphere isolated and homogenized, and an enriched cytosolic protein fraction was obtained by differential centrifugation. Naïve animals served as control. Immunoblotting for HMGB1 demonstrated a significant increase in cytosolic HMGB1 at 24 h in injured animals versus control ( $p < 0.0001$ ) (Fig. 1).

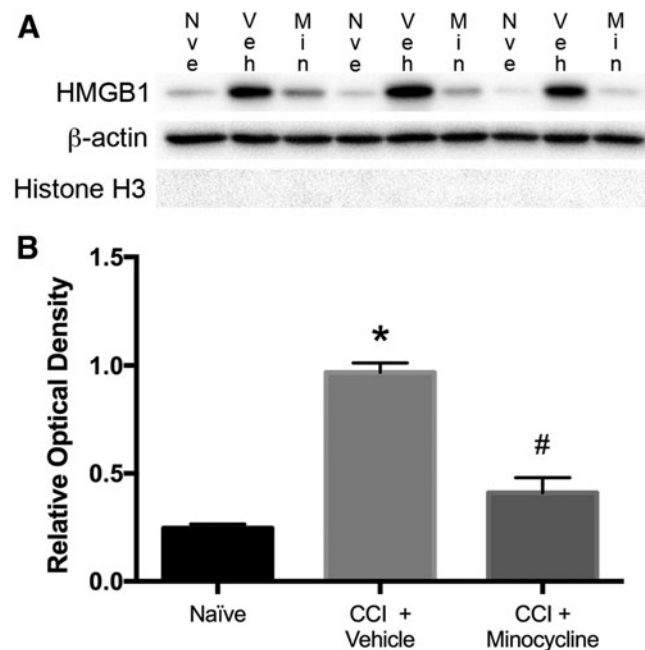


**FIG. 1.** Minocycline attenuates translocation of high mobility group box-1 (HMGB1) after traumatic brain injury in post-natal day 17 rats. (A) Western blot showing cytosolic fraction of homogenized ipsilateral hemisphere ( $20\text{-}\mu\text{g/well}$ ) from naïve, controlled cortical impact (CCI) + vehicle, and CCI + minocycline (90 mg/kg ip) treated rats 24 h after CCI. Blots were probed for HMGB1 with  $\beta$ -actin as loading control and Histone H3 to detect nuclear protein contamination. (B) Semiquantitative densitometry showing that CCI significantly increased HMGB1 in cytosolic fraction, and this effect was attenuated by treatment with minocycline. ( $n=3\text{--}4/\text{group}$ ). Data were analyzed by *t* test. \*  $p < 0.0001$  naïve vs. CCI + vehicle. #  $p < 0.001$  CCI + vehicle vs. CCI + minocycline. Graph shows mean + standard error of the mean.

Treatment with minocycline significantly reduced cytosolic HMGB1 in injured rats (CCI + vehicle  $3.81 \pm 0.17$  vs. CCI + minocycline  $1.62 \pm 0.27$ ;  $p < 0.001$ ). No significant difference in cytosolic HMGB1 was seen between naïve and minocycline-treated injured rats (naïve  $1.0 \pm 0.1$  vs. CCI + minocycline  $1.62 \pm 0.27$ ;  $p = 0.12$ ). In addition, we did not detect Histone H3 in the cytosolic fraction indicating minimal nuclear protein contamination.

#### Microglial response after TBI in PND 17 rats and the effect of minocycline

The peak time of the microglial response after TBI is unclear in pediatric TBI; however, studies in adult mice with CCI have suggested an initial peak on post-injury day 7.<sup>27</sup> To investigate the effect of minocycline on microglial activation after pediatric TBI, we performed Iba-1 immunohistochemistry to identify activated microglia in PND 17 rats seven days after CCI. Iba-1 immunoreactive microglia showed a ramified form in the naïve group (Fig. 2). In injured animals, treatment with minocycline produced a significant reduction in the number of Iba-1 positive objects in all brain regions assessed including hippocampus ( $595 \pm 110$  vs.  $2341 \pm 647$ ), cortex ( $1103 \pm 181$  vs.  $3076 \pm 502$ ), and thalamus ( $1348 \pm 233$  vs.  $2679 \pm 149$ ; all  $p < 0.05$  vs. vehicle). In addition, qualitatively, the microglial morphology in minocycline-treated animals appeared to be more ramified than in vehicle-treated rats.

#### Effect of minocycline on neuronal death after TBI in PND 17 rats

To evaluate the effect of minocycline on neurodegeneration after pediatric TBI, we performed FJB staining on coronal sections taken through the dorsal hippocampus in animals sacrificed seven days after injury. Given that in CCI, the cortex is severely damaged and results in a cavitory lesion, we focused our assessment of neuronal death on the underlying hippocampus and thalamus. The FJB-positive neurons were observed in both hippocampus and thalamus seven days after CCI versus control ( $p < 0.05$ ). In the hippocampus, no difference was seen in FJB-positive neurons between vehicle-treated and minocycline-treated animals.

In contrast to the hippocampus, we observed a significantly greater number of FJB-positive thalamic neurons in vehicle-treated animals than in minocycline-treated rats ( $78 \pm 6$  vs.  $442 \pm 66$  FJB-positive cells;  $p < 0.01$ ). (Fig. 3). Thus, to further quantify the effect of minocycline on neuronal degeneration in the thalamus, we performed unbiased stereology on cresyl violet stained coronal sections taken through the lesion in separate rats allowed to survive out to 14 days after injury to determine the number of surviving neurons. Injured animals had a significant decrease in thalamic neurons ipsilateral to CCI versus naïve (naïve  $22773 \pm 1012$  cells/mm<sup>3</sup> vs. CCI + vehicle  $11753 \pm 464$ ;  $p < 0.001$ ). The neuronal loss after CCI was attenuated

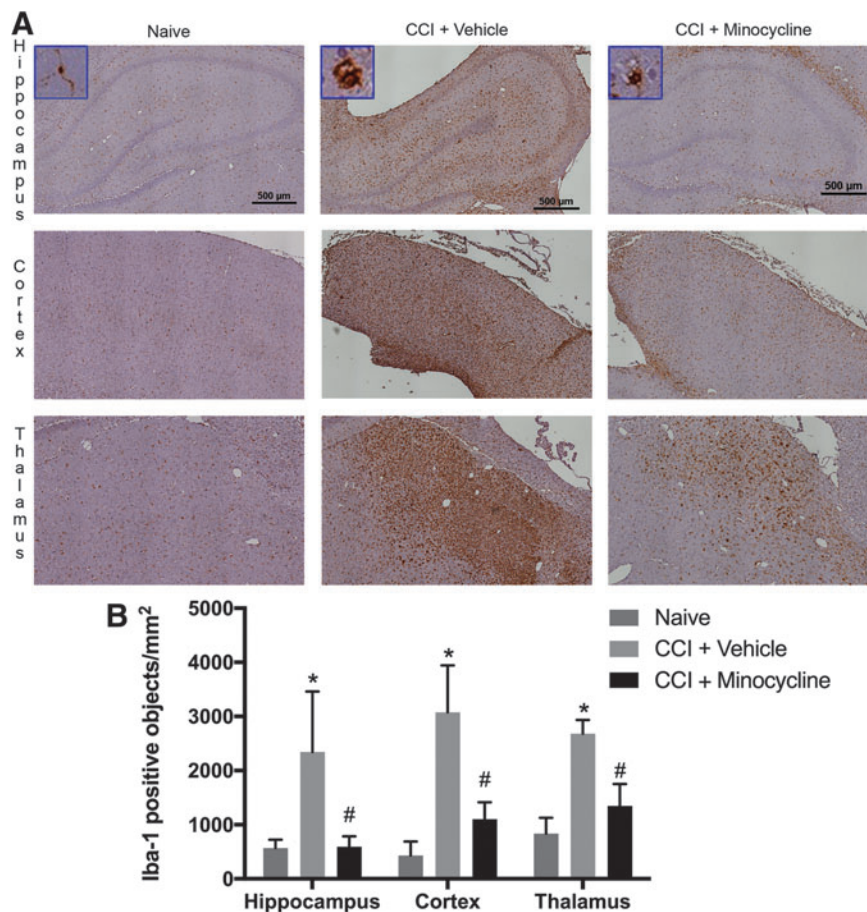


**FIG. 2.** Minocycline reduces microglial activation after traumatic brain injury in post-natal day 17 rats. (A) Rats were randomized to treatment with minocycline (90 mg/kg) or vehicle after controlled cortical impact (CCI) with naïve rats as control. At seven days after injury, animals were sacrificed for immunohistochemistry ( $n = 3$ /group). Shown are representative coronal sections at approximately  $-3.0$  to  $4.5$  mm bregma stained with anti-Iba-1. Insets include higher-magnification image of representative Iba-1 positive microglia. (B) Quantification of Iba-1 positive objects ( $n = 3$ /group). Data were analyzed by *t* test. \*  $p < 0.05$  naïve vs. CCI + vehicle. #  $p < 0.05$  CCI + vehicle vs. CCI + minocycline. Graph shows mean + standard error of the mean.

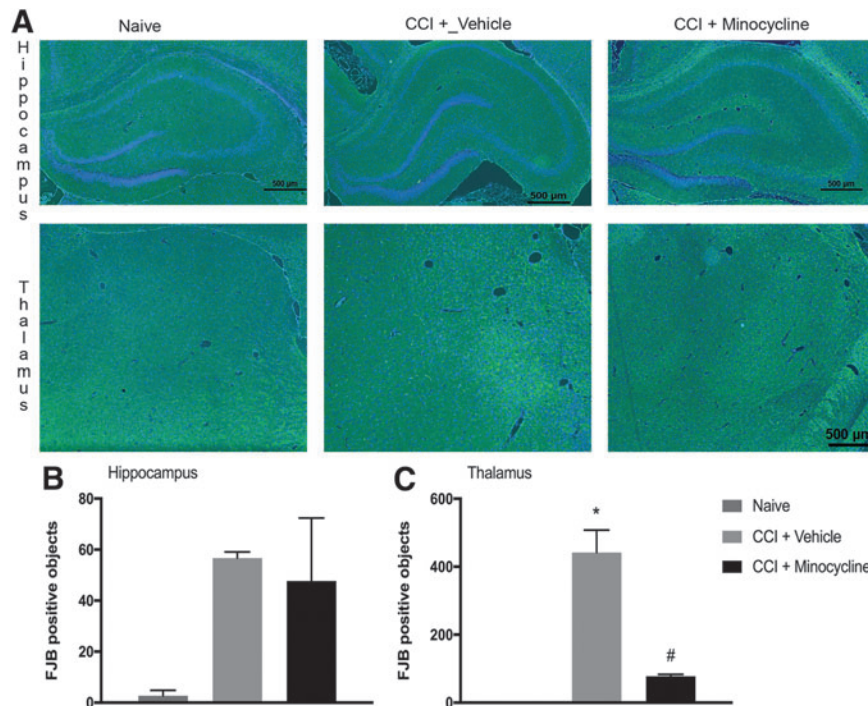


**FIG. 3.** Minocycline reduces neuronal degeneration in thalamus after traumatic brain injury in post-natal day 17 rats. (A) Rats were randomized to treatment with minocycline (90 mg/kg) or vehicle after controlled cortical impact (CCI) with naïve rats as control. At seven days after injury, animals were sacrificed for immunofluorescence ( $n=3/\text{group}$ ). Shown are representative coronal sections at approximately  $-3.0$  to  $4.5$  mm bregma stained Fluoro-Jade B (FJB). (B) Quantification of FJB positive cells ( $n=3/\text{group}$ ). Data were analyzed by  $t$  test. \*  $p<0.05$  naïve vs. CCI + vehicle. #  $p<0.05$  CCI + vehicle vs. CCI + minocycline. Graph shows mean + standard error of the mean.

by treatment with minocycline (CCI + vehicle  $11753 \pm 464$  vs. CCI + minocycline  $17047 \pm 524$ ;  $p<0.0001$ ) (Fig. 4).

Contrasting the effect of minocycline on neuronal death in thalamus, no significant difference was observed in lesion volume (Fig. 5), reflecting largely cortical tissue loss in this model.

#### Effect of minocycline on functional outcome after TBI in PND17 rats

Motor function was assessed by beam balance and incline plane test performed on post-injury days 1–5 (Fig. 6A,B). There were no significant effects in motor function task performance between sham and CCI-vehicle rats at this injury level. Minocycline-treated rats after CCI, however, showed poorer performance (reduced latency to fall) on beam balance (day 1:  $43 \pm 3$  vs.  $54 \pm 3$  sec;  $p<0.05$  vs. sham) and lower maximum angle on inclined plane (day 2:  $65 \pm 3$  vs.  $75 \pm 2$  degrees;  $p<0.05$  vs. sham). The minocycline-treated group recovered to sham-level performance by day 3 after injury.

Spatial memory acquisition was determined by MWM task on post-injury days 10–14 (Fig. 6C). Contrasting the detrimental effect on recovery of motor deficits in the early period after TBI, rats treated with minocycline showed a modest beneficial effect on MWM: CCI-vehicle treated rats exhibited a longer latency to find the hidden platform than sham animals on MWM (day 13:  $66 \pm 12$  vs.  $31 \pm 7$  sec | day 14:  $57 \pm 13$  vs.  $21 \pm 3$ ; all  $p<0.05$ ), but there was no difference between sham versus CCI–minocycline-treated rats on any days tested.

#### Discussion

In a model of pediatric TBI, we found treatment with minocycline attenuated translocation of the danger signal HMGB1 into the

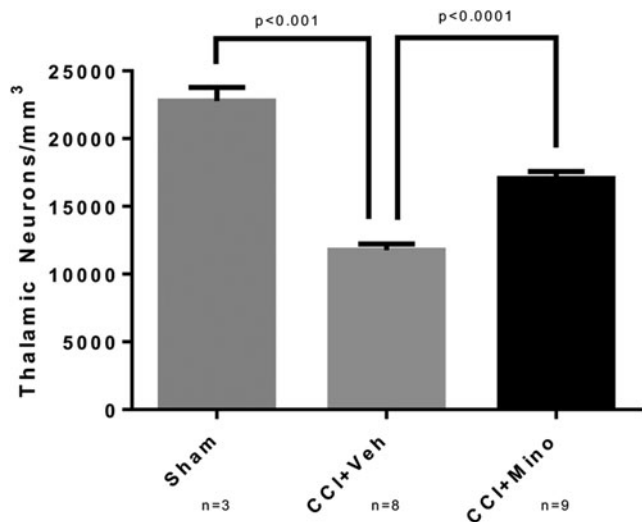


**FIG. 4.** Increased thalamic neurons after traumatic brain injury in post-natal day 17 rats treated with minocycline. Rats were randomized to treatment with minocycline (90 mg/kg) or vehicle after controlled cortical impact (CCI) with sham rats receiving anesthesia and craniotomy without CCI. At 14 days after injury, after completion of behavioral testing, rats were sacrificed and the brain harvested for neuronal counts by unbiased stereology. Injured rats had significant reduction in thalamic neurons (naïve  $22773 \pm 1012$  cells/mm<sup>3</sup> vs. CCI + vehicle  $11753 \pm 464$ ;  $p<0.001$ ). Thalamic neuronal loss after CCI was reduced by minocycline (CCI + vehicle  $11753 \pm 464$  vs. CCI + minocycline  $17047 \pm 524$ ;  $p<0.0001$ ).

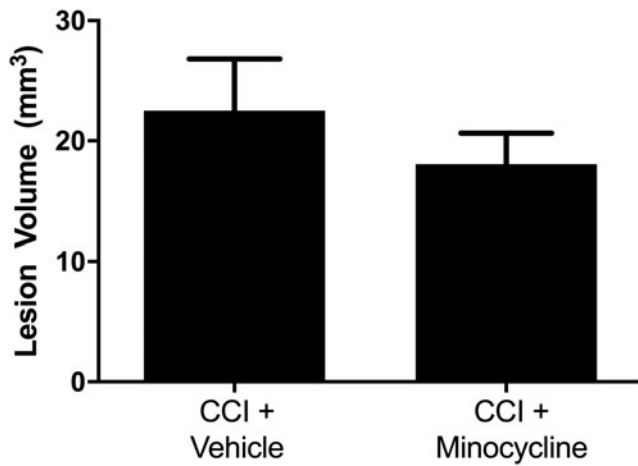


**FIG. 5.** No change in lesion volume after traumatic brain injury in post-natal day 17 rats treated with minocycline. Rats were randomized to treatment with minocycline (90 mg/kg) or vehicle after controlled cortical impact (CCI). Rats were sacrificed on day 14, and serial sections were taken through the lesion and analyzed with MCID image analysis software. No difference was seen between vehicle- and minocycline-treated groups (CCI + vehicle  $22.52 \pm 4.29 \text{ mm}^3$  vs. CCI + minocycline  $18.07 \pm 2.58 \text{ mm}^3$ ;  $p=0.32$ )

cytoplasm and produced a global reduction in post-injury microglial activation. In contrast, minocycline-induced neuroprotection was restricted to the thalamus in this model. Consistent with an overall beneficial effect of minocycline treatment, we also observed modestly improved spatial memory acquisition assessed out to two weeks after injury, despite delayed recovery of motor function after TBI with minocycline treatment. This report provides evidence for minocycline as a potential therapeutic agent for reducing neuroinflammation, targeting thalamic injury, and improving cognitive outcomes in pediatric TBI.

Microglia, the primary resident immune cells of the brain, become activated after TBI by the release of DAMPs.<sup>10</sup> Microglial activation after TBI is influenced by age, with patients at the extremes of age being prone to increased microglial activation and secondary brain injury.<sup>4,28</sup> In children with severe TBI, Newell and associates<sup>4</sup> found increased CSF ferritin, a marker of activated microglia and macrophages, was associated with age less than four years and unfavorable GOS score at six months. Inhibition of microglial activation, which has been proposed as a neuroprotective strategy, may therefore be more beneficial to younger children (and the elderly) after TBI.

HMGB1, a prototypical DAMP, is a DNA binding protein that may be released from the nucleus by traumatic lysis or necrotic cell death. In addition, in response to cell stress, HMGB1 becomes hyperacetylated and can translocate from nucleus to cytoplasm where it is secreted or released by activation of inflammasomes and stimulates an immune response.<sup>29</sup> Preventing cellular depletion of HMGB1 may also be beneficial for regenerative processes. Merianda and colleagues<sup>30</sup> observed that axonal HMGB1 translation was increased in response to injury and was required for neurite outgrowth in dorsal root ganglion neurons. In adult rodent models of TBI, inhibition of HMGB1-mediated inflammation has been associated with decreased pro-inflammatory cytokine expression, decreased blood-brain barrier permeability, and improved functional outcome.<sup>11,24,31,32</sup> In children with severe TBI, Au and coworkers<sup>5</sup> measured HMGB1 in ventricular

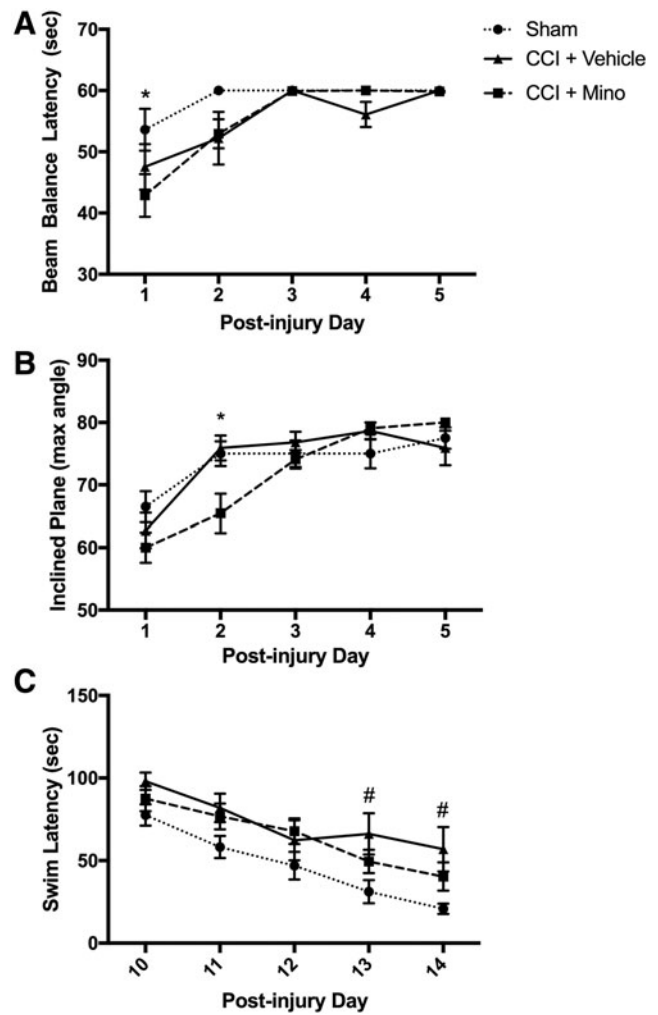


**FIG. 6.** Treatment with minocycline delays motor recovery and improves spatial memory acquisition after traumatic brain injury in post-natal day 17 rats. Rats were randomized to treatment with minocycline (90 mg/kg) or vehicle after controlled cortical impact (CCI) with sham rats receiving anesthesia and craniotomy without CCI ( $n=10-11/\text{group}$ ). (A) After CCI, rats treated with minocycline had reduced beam balance latency (day 1:  $43 \pm 3$  vs.  $54 \pm 3$  sec;  $p < 0.05$  vs. sham) and (B) reduced maximum angle on inclined plane (day 2:  $65 \pm 3$  vs.  $75 \pm 2$  degrees;  $p < 0.05$  vs. sham). No differences in motor function were observed between sham and CCI + vehicle groups. (C) Morris Water Maze was performed on day 10–14 after injury. On the final two days of testing, vehicle-treated rats had increased latency compared with shams (day 13:  $66 \pm 12$  vs.  $31 \pm 7$  sec | day 14:  $57 \pm 13$  vs.  $21 \pm 3$ ; all  $p < 0.05$ ); there was no difference between sham vs. CCI.

CSF and observed a significant inverse correlation between peak HMGB1 concentration and six-month GOS score.

There are several mechanisms by which minocycline may reduce extracellular HMGB1.<sup>33,34</sup> Minocycline at nanomolar concentrations has been shown to inhibit poly(ADP-ribose) polymerase-1 (PARP-1), an NAD-dependent DNA repair enzyme.<sup>35</sup> By blocking PARP-1 activity after TBI, minocycline may prevent cellular necrosis and passive release of HMGB1. In addition, PARP-1 inhibition has been shown to preserve the activity of NAD-dependent histone deacetylases, promote deacetylation of HMGB1 and retention in the nucleus.<sup>36</sup> HMGB1 release is also

regulated by the inflammasome and pyroptosis, or caspase-1 dependent cell death.

Reactive oxygen species generation is thought to be a common pathway for multiple inflammasome triggers<sup>37</sup> and may be blocked by the downstream antioxidant consequences of minocycline. In addition, minocycline was shown in a study by Sanchez Mejia and colleagues<sup>16</sup> to reduce the activity of caspase-1 after TBI in adult mice that received a similar dosing regimen to our study, except the mice were also pre-treated with minocycline 12 h before injury. The dose used in our study, 90 mg/kg ip at 10 min and 20 h post-injury is higher than was used in some of the neonatal and adult models, and many different doses have been used in pre-clinical and clinical testing with minocycline. We based the dosing regimen on the study by Sanchez Mejia and colleagues,<sup>16</sup> a study by Tang and associates<sup>38</sup> demonstrating neuroprotection after asphyxial cardiac arrest in PND 17 rats treated with 90 mg/kg ip dose, and the pharmacokinetic studies by Fagan and associates.<sup>39</sup> Although additional work needs to be done on dose response for this agent and others targeting HMGB1, we were able to demonstrate global effects on HMGB1 translocation and microglial response in our model.

Our findings contribute to two recently published studies of minocycline in neonatal TBI models. Hanlon and coworkers<sup>18</sup> studied minocycline in a repetitive closed-head injury model in PND 11 rats using a dose of 45 mg/kg ip every 12 h for three days. In contrast to our study, there was no effect of minocycline on microglial activation in the cortex, hippocampus, or thalamus using this dosing regimen and injury model. The investigators observed a modest reduction in microglia in the corpus callosum that was not associated with changes in axonal injury or MWM swim latency. Chhor and colleagues<sup>19</sup> used PND 7 rats in a single impact closed-head diffuse injury model. Minocycline (45 mg/kg) was given immediately after injury and then daily for an additional two days. The investigators found reduced apoptotic cell death in the cortex, hippocampus, and striatum in animals treated with minocycline without significant change in the lesion evaluated at five days. Although no difference was seen in the number of activated microglia, Iba-1 was assessed early (one day post-injury) which might account for the difference with our results. Microglia were isolated for gene expression analysis, which showed mixed results such as a decrease in pro-inflammatory interleukin (IL)-6 gene expression and increase in pro-inflammatory IL-1 $\beta$  gene expression.

Overall, these studies do not show a strong benefit for minocycline treatment in the neonatal TBI population with single or repetitive head injury. There are important and robust age-related differences, however, in the response to brain injury between 7 and 17 days in rats, and issues such as dosing, timing of administration, injury severity, and brain region assessed could also impact the findings. Indeed, findings in neonatal and pediatric brain injury models are desperately needed to better develop age appropriate targeted therapies for TBI.

Our data are novel in that, despite global effects on the microglial response, minocycline treatment produced a selective albeit robust attenuation of neuronal death in the thalamus. Although MWM performance is typically associated with lesions in the hippocampus, thalamic nuclei may also play a role and have contributed to our findings.<sup>40</sup> The thalamus is a very heterogeneous structure, and cell death mechanisms likely differ between various thalamic nuclei as Bramlett and coworkers<sup>41</sup> demonstrated in a fluid percussion model. Apoptotic cell death in the thalamus may be delayed, peaking up to two weeks after trauma in adult mice. In the developing rat brain, Bittigau and associates<sup>42</sup> used TUNEL

staining and electron microscopy to identify apoptotic cells after a weight drop model and observed apoptotic degeneration out to five days post-injury in the dorsolateral thalamus. These diaschisis lesions were described recently by Wiley and coworkers<sup>43</sup> and may be reversible by the antiapoptotic effects of minocycline.

Thalamic injury after TBI may lead to a condition called chronic paroxysmal sympathetic hyperactivity (PSH). In 2014, criteria were developed to describe PSH in survivors of severe acquired brain injury with paroxysmal increases in sympathetic tone and muscle rigidity.<sup>44</sup> Symptoms of PSH occur in 8–33% of adults after TBI<sup>45</sup> and are associated with poor outcome. Kirk and associates<sup>46</sup> observed a prevalence of 13% incidence in children with acquired brain injury (10% of children with TBI) associated with longer hospitalization and worse neurobehavioral outcomes. Whether minocycline is able to ameliorate these symptoms by reducing thalamic neuronal death may be an area for future research.

The clinical use of minocycline in children may be hampered by concerns of staining dental enamel by the tetracycline class of antibiotics. Minocycline is currently not recommended in children until 8 years of age, when the majority of mineralization of succedaneous teeth has occurred. In an observational cohort study of children treated with minocycline, however, Cascio and colleagues<sup>47</sup> reported no increase in incidence of enamel staining. Alternative interventions to attenuate microglial activation and HMGB1 translocation with different side effect profiles may be preferable in young children.

## Conclusion

Our findings are consistent with minocycline reducing the neuroinflammatory response to pediatric TBI, including HMGB-1 translocation and microglial activation. In addition, we observed a novel regional neuroprotective effect in the thalamus and improved cognitive outcomes. Further study is needed to characterize each of these effects including their mechanistic underpinning and implications to long-term outcome in pediatric TBI.

## Acknowledgment

Support was received from NINDS grants R01 NS38620 and U01 NS081041; and NICHD T32 HD40686.

## Author Disclosure Statement

No competing financial interests exist.

## References

1. Coronado, V.G., Xu, L., Basavaraju, S.V., McGuire, L.C., Wald, M.M., Faul, M.D., Guzman, B.R., Hemphill, J.D. Centers for Disease Control and Prevention (2011). Surveillance for traumatic brain injury-related deaths—United States, 1997–2007. *MMWR Surveill. Summ.* 60, 1–32.
2. Cernak, I., Chang, T., Ahmed, F.A., Cruz, M.I., Vink, R., Stoica, B., and Faden, A.I. (2010). Pathophysiological response to experimental diffuse brain trauma differs as a function of developmental age. *Dev. Neurosci.* 32, 442–453.
3. Morrison, W.E., Arbelaez, J.J., Fackler, J.C., De Maio, A., and Paidas, C.N. (2004). Gender and age effects on outcome after pediatric traumatic brain injury. *Pediatr. Crit. Care Med.* 5, 145–151.
4. Newell, E., Shellington, D.K., Simon, D.W., Bell, M.J., Kochanek, P.M., Feldman, K., Bayir, H., Aneja, R.K., Carcillo, J.A., and Clark, R.S. (2015). Cerebrospinal fluid markers of macrophage and lymphocyte activation after traumatic brain injury in children. *Pediatr. Crit. Care Med.* 16, 549–557.
5. Au, A.K., Aneja, R.K., Bell, M.J., Bayir, H., Feldman, K., Adelson, P.D., Fink, E.L., Kochanek, P.M., and Clark, R.S. (2012). Cere-

- brospinal fluid levels of high-mobility group box 1 and cytochrome C predict outcome after pediatric traumatic brain injury. *J. Neurotrauma* 29, 2013–2021.
6. Wallisch, J.S., Simon, D.W., Bayir, H., Bell, M.J., Kochanek, P.M., and Clark, R.S. (2017). Cerebrospinal fluid NLRP3 is increased after severe traumatic brain injury in infants and children. *Neurocrit. Care*. Epub ahead of print.
  7. Simon, D.W., McGeachy, M.J., Bayir, H., Clark, R.S., Loane, D.J., and Kochanek, P.M. (2017). The far-reaching scope of neuroinflammation after traumatic brain injury. *Nat. Rev. Neurol.* 13, 171–191.
  8. Bell, M.J., Kochanek, P.M., Doughty, L.A., Carcillo, J.A., Adelson, P.D., Clark, R.S., Wisniewski, S.R., Whalen, M.J., and DeKosky, S.T. (1997). Interleukin-6 and interleukin-10 in cerebrospinal fluid after severe traumatic brain injury in children. *J. Neurotrauma* 14, 451–457.
  9. Satchell, M.A., Lai, Y., Kochanek, P.M., Wisniewski, S.R., Fink, E.L., Siedberg, N.A., Berger, R.P., DeKosky, S.T., Adelson, P.D., and Clark, R.S. (2005). Cytochrome c, a biomarker of apoptosis, is increased in cerebrospinal fluid from infants with inflicted brain injury from child abuse. *J. Cereb. Blood Flow Metab.* 25, 919–927.
  10. Loane, D.J. and Byrnes, K.R. (2010). Role of microglia in neurotrauma. *Neurotherapeutics* 7, 366–377.
  11. Laird, M.D., Shields, J.S., Sukumari-Ramesh, S., Kimbler, D.E., Fessler, R.D., Shakir, B., Youssef, P., Yanasak, N., Vender, J.R., and Dhandapani, K.M. (2014). High mobility group box protein-1 promotes cerebral edema after traumatic brain injury via activation of toll-like receptor 4. *Glia* 62, 26–38.
  12. Andersson, U. and Tracey, K.J. (2011). HMGB1 is a therapeutic target for sterile inflammation and infection. *Annu Rev. Immunol.* 29, 139–162.
  13. Homsy, S., Piaggio, T., Croci, N., Noble, F., Plotkine, M., Marchand-Leroux, C., and Jafarian-Tehrani, M. (2010). Blockade of acute microglial activation by minocycline promotes neuroprotection and reduces locomotor hyperactivity after closed head injury in mice: a twelve-week follow-up study. *J. Neurotrauma* 27, 911–921.
  14. Kovsdi, E., Kamnakh, A., Wingo, D., Ahmed, F., Grunberg, N.E., Long, J.B., Kasper, C.E., and Agoston, D.V. (2012). Acute minocycline treatment mitigates the symptoms of mild blast-induced traumatic brain injury. *Front. Neurol.* 3, 111.
  15. Bye, N., Habgood, M.D., Callaway, J.K., Malakooti, N., Potter, A., Kossmann, T., and Morganti-Kossmann, M.C. (2007). Transient neuroprotection by minocycline following traumatic brain injury is associated with attenuated microglial activation but no changes in cell apoptosis or neutrophil infiltration. *Exp. Neurol.* 204, 220–233.
  16. Sanchez Mejia, R.O., Ona, V.O., Li, M., and Friedlander, R.M. (2001). Minocycline reduces traumatic brain injury-mediated caspase-1 activation, tissue damage, and neurological dysfunction. *Neurosurgery* 48, 1393–1399.
  17. Siopi, E., Llufrui-Daben, G., Fanucchi, F., Plotkine, M., Marchand-Leroux, C., and Jafarian-Tehrani, M. (2012). Evaluation of late cognitive impairment and anxiety states following traumatic brain injury in mice: the effect of minocycline. *Neurosci. Lett.* 511, 110–115.
  18. Hanlon, L.A., Huh, J.W., and Raghupathi, R. (2016). Minocycline transiently reduces microglia/macrophage activation but exacerbates cognitive deficits following repetitive traumatic brain injury in the neonatal rat. *J. Neuropathol. Exp. Neurol.* 75, 214–226.
  19. Chhor, V., Moretti, R., Le Charpentier, T., Sigaut, S., Lebon, S., Schwendimann, L., Ore, M.V., Zuiani, C., Milan, V., Jossierand, J., Vontell, R., Pansiot, J., Degos, V., Ikonomidou, C., Titomanlio, L., Hagberg, H., Gressens, P., and Fleiss, B. (2017). Role of microglia in a mouse model of paediatric traumatic brain injury. *Brain Behav. Immun.* 63, 197–209.
  20. Hayakawa, K., Mishima, K., Nozako, M., Hazekawa, M., Mishima, S., Fujioka, M., Orito, K., Egashira, N., Iwasaki, K., and Fujiwara, M. (2008). Delayed treatment with minocycline ameliorates neurologic impairment through activated microglia expressing a high-mobility group box1-inhibiting mechanism. *Stroke* 39, 951–958.
  21. Kikuchi, K., Kawahara, K., Biswas, K.K., Ito, T., Tancharoen, S., Morimoto, Y., Matsuda, F., Oyama, Y., Takenouchi, K., Miura, N., Arimura, N., Nawa, Y., Meng, X., Shrestha, B., Arimura, S., Iwata, M., Mera, K., Sameshima, H., Ohno, Y., Maenosono, R., Yoshida, Y., Tajima, Y., Uchikado, H., Kuramoto, T., Nakayama, K., Shigemori, M., Hashiguchi, T., and Maruyama, I. (2009). Minocycline attenuates both OGD-induced HMGB1 release and HMGB1-induced cell death in ischemic neuronal injury in PC12 cells. *Biochem. Biophys. Res. Commun.* 385, 132–136.
  22. Hu, X., Zhou, X., He, B., Xu, C., Wu, L., Cui, B., Wen, H., Lu, Z., and Jiang, H. (2010). Minocycline protects against myocardial ischemia and reperfusion injury by inhibiting high mobility group box 1 protein in rats. *Eur. J. Pharmacol.* 638, 84–89.
  23. Jenkins, L.W., Peters, G.W., Dixon, C.E., Zhang, X., Clark, R.S., Skinner, J.C., Marion, D.W., Adelson, P.D., and Kochanek, P.M. (2002). Conventional and functional proteomics using large format two-dimensional gel electrophoresis 24 hours after controlled cortical impact in postnatal day 17 rats. *J. Neurotrauma* 19, 715–740.
  24. Okuma, Y., Liu, K., Wake, H., Zhang, J., Maruo, T., Date, I., Yoshino, T., Ohtsuka, A., Otani, N., Tomura, S., Shima, K., Yamamoto, Y., Yamamoto, H., Takahashi, H.K., Mori, S., and Nishibori, M. (2012). Anti-high mobility group box-1 antibody therapy for traumatic brain injury. *Ann. Neurol.* 72, 373–384.
  25. Whalen, M.J., Carlos, T.M., Dixon, C.E., Schiding, J.K., Clark, R.S., Baum, E., Yan, H.Q., Marion, D.W., and Kochanek, P.M. (1999). Effect of traumatic brain injury in mice deficient in intercellular adhesion molecule-1: assessment of histopathologic and functional outcome. *J. Neurotrauma* 16, 299–309.
  26. Kabadi, S.V., Stoica, B.A., Hanscom, M., Loane, D.J., Kharebava, G., Murray II, M.G., Cabatbat, R.M., and Faden, A.I. (2012). CR8, a selective and potent CDK inhibitor, provides neuroprotection in experimental traumatic brain injury. *Neurotherapeutics* 9, 405–421.
  27. Jin, X., Ishii, H., Bai, Z., Itokazu, T., and Yamashita, T. (2012). Temporal changes in cell marker expression and cellular infiltration in a controlled cortical impact model in adult male C57BL/6 mice. *PLoS One* 7, e41892.
  28. Kumar, A., Stoica, B.A., Sabirzhanov, B., Burns, M.P., Faden, A.I., and Loane, D.J. (2013). Traumatic brain injury in aged animals increases lesion size and chronically alters microglial/macrophage classical and alternative activation states. *Neurobiol. Aging* 34, 1397–1411.
  29. Lu, B., Wang, H., Andersson, U., and Tracey, K.J. (2013). Regulation of HMGB1 release by inflammasomes. *Protein Cell* 4, 163–167.
  30. Merianda, T.T., Coleman, J., Kim, H.H., Kumar Sahoo, P., Gomes, C., Brito-Vargas, P., Rauvala, H., Blesch, A., Yoo, S., and Twiss, J.L. (2015). Axonal amphoterin mRNA is regulated by translational control and enhances axon outgrowth. *J. Neurosci.* 35, 5693–5706.
  31. Su, X., Wang, H., Zhao, J., Pan, H., and Mao, L. (2011). Beneficial effects of ethyl pyruvate through inhibiting high-mobility group box 1 expression and TLR4/NF-kappaB pathway after traumatic brain injury in the rat. *Mediators Inflamm.* 2011, 807142.
  32. Okuma, Y., Liu, K., Wake, H., Liu, R., Nishimura, Y., Hui, Z., Teshigawara, K., Haruma, J., Yamamoto, Y., Yamamoto, H., Date, I., Takahashi, H.K., Mori, S., and Nishibori, M. (2014). Glycyrrhizin inhibits traumatic brain injury by reducing HMGB1-RAGE interaction. *Neuropharmacology* 85, 18–26.
  33. Elewa, H.F., Hilali, H., Hess, D.C., Machado, L.S., and Fagan, S.C. (2006). Minocycline for short-term neuroprotection. *Pharmacotherapy* 26, 515–521.
  34. Plane, J.M., Shen, Y., Pleasure, D.E., and Deng, W. (2010). Prospects for minocycline neuroprotection. *Arch. Neurol.* 67, 1442–1448.
  35. Alano, C.C., Kauppinen, T.M., Valls, A.V., and Swanson, R.A. (2006). Minocycline inhibits poly(ADP-ribose) polymerase-1 at nanomolar concentrations. *Proc. Natl. Acad. Sci. U. S. A.* 103, 9685–9690.
  36. Walko, T.D., 3rd, Di Caro, V., Piganelli, J., Billiar, T.R., Clark, R.S., and Aneja, R.K. (2015). Poly(ADP-ribose) polymerase 1-sirtuin 1 functional interplay regulates LPS-mediated high mobility group box 1 secretion. *Mol. Med.* 20, 612–624.
  37. de Rivero Vaccari, J.P., Dietrich, W.D., and Keane, R.W. (2014). Activation and regulation of cellular inflammasomes: gaps in our knowledge for central nervous system injury. *J. Cereb. Blood Flow Metab.* 34, 369–375.
  38. Tang, M., Alexander, H., Clark, R.S., Kochanek, P.M., Kagan, V.E., and Bayir, H. (2010). Minocycline reduces neuronal death and attenuates microglial response after pediatric asphyxial cardiac arrest. *J. Cereb. Blood Flow Metab.* 30, 119–129.
  39. Fagan, S.C., Edwards, D.J., Borlongan, C.V., Xu, L., Arora, A., Feuerstein, G., and Hess, D.C. (2004). Optimal delivery of minocycline to the brain: implication for human studies of acute neuroprotection. *Exp. Neurol.* 186, 248–251.



40. Stackman, R.W., Jr., Lora, J.C., and Williams, S.B. (2012). Directional responding of C57BL/6J mice in the Morris water maze is influenced by visual and vestibular cues and is dependent on the anterior thalamic nuclei. *J. Neurosci.* 32, 10211–10225.
41. Bramlett, H.M., Dietrich, W.D., Green, E.J., and Busto, R. (1997). Chronic histopathological consequences of fluid-percussion brain injury in rats: effects of post-traumatic hypothermia. *Acta Neuropathol.* 93, 190–199.
42. Bittigau, P., Sifringer, M., Pohl, D., Stadthaus, D., Ishimaru, M., Shimizu, H., Ikeda, M., Lang, D., Speer, A., Olney, J.W., and Ikonomidou, C. (1999). Apoptotic neurodegeneration following trauma is markedly enhanced in the immature brain. *Ann Neurol* 45, 724–735.
43. Wiley, C.A., Bissel, S.J., Lesniak, A., Dixon, C.E., Franks, J., Beer Stolz, D., Sun, M., Wang, G., Switzer, R., Kochanek, P.M., and Murdoch, G. (2016). Ultrastructure of diaschisis lesions after traumatic brain injury. *J. Neurotrauma* 33, 1866–1882.
44. Baguley, I.J., Perkes, I.E., Fernandez-Ortega, J.F., Rabinstein, A.A., Dolce, G., and Hendricks, H.T. (2014). Paroxysmal sympathetic hyperactivity after acquired brain injury: consensus on conceptual definition, nomenclature, and diagnostic criteria. *J Neurotrauma* 31, 1515–1520.
45. Baguley, I.J., Heriseanu, R.E., Cameron, I.D., Nott, M.T., and Slew-Younan, S. (2008). A critical review of the pathophysiology of dysautonomia following traumatic brain injury. *Neurocrit. Care* 8, 293–300.
46. Kirk, K.A., Shoykhet, M., Jeong, J.H., Tyler-Kabara, E.C., Henderson, M.J., Bell, M.J., and Fink, E.L. (2012). Dystautonomia after pediatric brain injury. *Dev Med Child Neurol.* 54, 759–764.
47. Cascio, A., Di Liberto, C., D'Angelo, M., Iaria, C., Scarlata, F., Titone, L., and Campisi, G. (2004). No findings of dental defects in children treated with minocycline. *Antimicrob Agents Chemother.* 48, 2739–2741.

Address correspondence to:

*Dennis W. Simon, MD*

*Children's Hospital of Pittsburgh*

*4401 Penn Avenue*

*Pittsburgh, PA 15224*

*E-mail: dennis.simon2@chp.edu*